LUND UNIVERSITY

Laser-Induced Incandescence for Soot Particle Size Measurements in Premixed Flat Flames

Axelsson, Boman; Collin, Robert; Bengtsson, Per-Erik

Published in:
Applied Optics

DOI:
10.1364/AO.39.003683

2000

Link to publication

Citation for published version (APA):
Axelsson, B., Collin, R., & Bengtsson, P.-E. (2000). Laser-Induced Incandescence for Soot Particle Size Measurements in Premixed Flat Flames. *Applied Optics*, *39*(21), 3683-3690. https://doi.org/10.1364/AO.39.003683

Total number of authors:
3

General rights
Unless other specific re-use rights are stated the following general rights apply:
Copyright and moral rights for the publications made accessible in the public portal are retained by the authors and/or other copyright owners and it is a condition of accessing publications that users recognise and abide by the legal requirements associated with these rights.
• Users may download and print one copy of any publication from the public portal for the purpose of private study or research.
• You may not further distribute the material or use it for any profit-making activity or commercial gain
• You may freely distribute the URL identifying the publication in the public portal

Read more about Creative commons licenses: https://creativecommons.org/licenses/

Take down policy
If you believe that this document breaches copyright please contact us providing details, and we will remove access to the work immediately and investigate your claim.

LUND UNIVERSITY

PO Box 117
221 00 Lund
+46 46-222 00 00

Laser-induced incandescence for soot particle size measurements in premixed flat flames

Boman Axelsson, Robert Collin, and Per-Erik Bengtsson

Measurements of soot properties by means of laser-induced incandescence (LII) and combined scattering–extinction were performed in well-characterized premixed ethylene–air flames. In particular, the possibility of using LII as a tool for quantitative particle sizing was investigated. Particle sizes were evaluated from the temporal decay of the LII signal combined with heat balance modeling of laser-heated particles, and these sizes were compared with the particle sizes deduced from scattering–extinction measurements based on isotropic sphere theory. The correspondence was good early in the soot-formation process but less good at later stages, possibly because aggregation to clusters began to occur. A critical analysis has been made of how uncertainties in different parameters, both experimental and in the model, affect the evaluated particle sizes for LII. A sensitivity analysis of the LII model identified the ambient-flame temperature as a major source of uncertainty in the evaluated particle size, a conclusion that was supported by an analysis based on temporal LII profiles. © 2000 Optical Society of America

OCIS codes: 140.3460, 280.1740, 280.2470.

1. Introduction

The incandescence from laser-heated soot particles was observed by Eckbreth in 1977.[1] At that time, the phenomenon was considered a problem in Raman measurements. However, during the past 15 years, use of the method of laser-induced incandescence (LII) to measure the properties of soot has been considered. During the past several years numerous studies and applications of LII have proved its utility as a diagnostic tool for measurements of both soot volume fraction and particle size.[2–18] Part of the increased interest in LII must be attributed to tightened particulate-emission standards. Meeting these standards will require a better understanding of soot formation and oxidation in combustion systems; thus there is a need for a new diagnostic tool with high spatial and temporal resolution. In this context LII has been used inside the cylinders of diesel engines, for example,[19] as well as in exhaust gas flows.[20] Although much progress on application of LII to practical combustion situations has been made, it is necessary to test the potential of the technique further and to identify basic limitations in well-characterized flames, for example, laminar flat flames burning on porous-plug burners. Flames on such a burner are easily probed with laser diagnostics, and each height represents a time in the soot-formation process.

We have used laser diagnostics to investigate laminar premixed ethylene–air flames. Flame temperatures were measured with rotational coherent anti-Stokes–Raman spectroscopy (CARS). Soot volume fractions were evaluated from measurements of laser-induced incandescence and extinction measurements, and soot particle sizes were evaluated from the temporal profile of the LII signal and combined Rayleigh scattering–extinction measurements. In this investigation we aim to explore further the ability of using the temporal profile of the LII signal for soot particle sizing; we discuss critical issues in the evaluation of particle sizes with both techniques.

2. Soot Diagnostic Fundamentals

A. Scattering–Extinction

The combined measurements of scattering and extinction have been widely used in determining soot volume fraction and soot particle size in both diffusion flames and premixed flames.[21–23] The calculation of soot properties is based on the Rayleigh theory

The authors are with the Division of Combustion Physics, Lund Institute of Technology, P.O. Box 118, S-221 00 Lund, Sweden. The e-mail address for B. Axelsson is boman.axelsson@forbrf.lth.se.

Received 24 September 1999; revised manuscript received 28 April 2000.

0003-6935/00/213683-08$15.00/0

© 2000 Optical Society of America

for isotropic spheres, in which the diameters of the spheres are much smaller than the laser wavelength. In this section, only relations that are important for the final conclusions are elucidated; the full theory can be found, for example, in Ref. 24. From the theory it is obvious that the soot volume fraction f_v can be extracted from an extinction measurement if the refractive index $\mathbf{m}$ is known:

$$f_v = \frac{\lambda}{6\pi}\frac{K_{\text{ext}}}{E(\mathbf{m})}, \qquad E(\mathbf{m}) = -\text{Im}\left(\frac{m^2-1}{m^2+2}\right), \tag{1}$$

where λ is the wavelength and K_{ext} the extinction coefficient. Further, if an elastic scattering measurement is made in an identical configuration, a measure of the soot particle diameter d_{es} can be evaluated:

$$d_{\text{es}} = \lambda\left(\frac{4}{\pi^2}\right)^{1/3}\left[\frac{E(\mathbf{m})}{F(\mathbf{m})}\right]^{1/3}\left(\frac{Q_{vv}}{K_{\text{ext}}}\right)^{1/3},$$
$$F(\mathbf{m}) = \left|\frac{\mathbf{m}^2-1}{\mathbf{m}^2+2}\right|^2. \tag{2}$$

The scattering factor Q_{vv} from a flame measurement is obtained from calibration measurements in gases with known cross sections, whereas K_{ext} is evaluated experimentally from an absorption measurement. Extinction caused by scattering is negligible for a particle in the Rayleigh regime, i.e., when the particle is much smaller than the laser wavelength, which makes the extinction coefficient equal to the absorption coefficient.

Equations (1) and (2) are valid for isotropic spheres in a monodisperse system with particle sizes much smaller than the laser wavelengths. Naturally, the theory is not totally applicable to an ensemble of soot particles in a flame, which we discuss throughout the paper. In the early stages of soot formation, just after nucleation, the assumptions of the theory are more valid than in later stages when the individual particles more likely tend to form aggregates of soot particles in the forms of chains and clusters. During this aging the size distribution becomes wider, and the composition of the soot particle changes toward a higher carbon content. Thus both uncertainty in the refractive index and the assumption of monodispersivity are limitations to the theory in its present form.

The particle diameter evaluated from a scattering–extinction measurement is called the volume-equivalent sphere diameter d_{es}. In flame regions where aggregation occurs, the calculated volume-equivalent diameter gives information about neither the soot aggregate structure nor the size of the primary particles that constitute the soot aggregate. References 14 and 25, e.g., describe investigations of the soot aggregate structures in which laser-heated soot was thermophoretically sampled and studied with transmission-electron microscopy.

B. Laser-Induced Incandescence

LII became a laser diagnostic technique for soot diagnostics after the pioneering research of Melton in 1984.[2] The use of LII makes it possible to make spatially and temporally resolved measurements of soot volume fraction in simple flames as well as in more-complex combustion systems.[19,26] Normally, laser light from a pulsed laser is directed through the flame, which results in rapid heating of particles to temperatures of 4000–4500 K. The detector could be a photomultiplier tube for point measurements or an image-intensified CCD for two-dimensional planar visualization. Important issues to consider for a LII measurement are the characteristics of the incident laser light, and the detection range, spectral as well as temporal. These issues have been thoroughly investigated; see, e.g., Refs. 3, 7, 13, and 27.

The choice of laser wavelength for LII is not critical, inasmuch as soot absorbs strongly in a large spectral region from the ultraviolet to the infrared. To prevent fluorescence interference to the LII signal from polyaromatic hydrocarbons, one should not use a laser wavelength in the ultraviolet.[6] Fluorescence from laser-produced C_2 radicals as a result of soot vaporization can be observed by use of laser wavelengths in resonance with the Swan bands of C_2. This signal can, however, under some circumstances also be used for soot diagnostics.[6] In most LII experiments either the fundamental wavelength 1064 nm or the second-harmonic wavelength at 532 nm of a Nd:YAG laser has been used as the laser source.

The choice of detection wavelength is somewhat more complex, because there are both advantages and disadvantages for a given choice. Calculations by Melton showed that the LII signal has a dependence on the soot particle diameter raised to a power of $(3 + 0.154/\lambda_{\text{det}})$, which favors the use of long detection wavelengths, λ_{det},[2] because the relationship between the LII signal and the soot volume fraction will thereby be improved. Also, if a short detection wavelength is used, the LII signal will be biased toward particles with higher final temperature, i.e., larger particles.[2,27] A shorter detection wavelength, however, will minimize the contribution from background flame emission to the LII signal, which can be a problem in applications in which background suppression is not possible and the flame is physically large.[28]

For the best proportionality to soot volume fraction, the detection gate should be prompt and not too long [~25–100 ns (Ref. 27)]. A delayed detection gate biases the LII measurements in favor of large particles.[2,7,27,29] Such is also true for long gate widths.[29] The detected LII signal has to be calibrated to give an absolute value of soot volume fraction. A well-characterized flame, for which the soot volume fractions have been calculated from, for example, extinction measurements, is often used for this purpose. The calibration is not a major problem in open configurations, but in, e.g., in-cylinder measurements, the calibration could be more complex.

The idea of using the temporal profile of the LII signal to determine particle size was proposed by Melton,[2] but the first published measurements were performed by Will *et al.*[9]; there the combination of measurement and modeling of the LII signal gave the particle size. The simple idea is that the temporal decay of the LII signal from a larger soot particle is longer than for a smaller soot particle. One can determine the temporal decay either by analyzing the curve directly[18,30] or by taking the ratio between the signals within two time gates.[13,17,18] The latter method has the advantage of making possible two-dimensional measurements of particle size.[17] Regardless of the method chosen, interpreting the detected signal in terms of particle size requires modeling. The evaluated particle size will be the primary particle size d_p,[13,31] unlike in scattering measurements, for which the volume-equivalent sphere diameter d_{es} is the measured quantity.

When the particle cools, the signal decreases, and in addition there is a wavelength shift of the signal. The decay time will thus depend not only on the particle size but also on the detection wavelength. Therefore it is necessary to know the transmission characteristics of optical components in the collection system. In the present investigation we selected a narrow spectral interval, using a narrow-band interference filter with a center wavelength of 400 nm and a bandwidth of 10 nm.

To evaluate a primary particle diameter from the measured temporal decay time of the LII signal requires a model for the particle cooling. The model that we used is the one proposed by Melton[2] in the form suggested by Will *et al.*[17]

3. Experiment

Measurements were made in two premixed ethylene–air flames burning on a sintered stainless-steel plug (a so-called McKenna burner) with a diameter of 60 mm.[32] The equivalence ratios of the two flames were 2.1 and 2.3, and both flames had a constant gas flow of 10 L/min (at 273 K and $p = 0.1$ MPa). The flame was stabilized with a steel plate, of the same diameter as the burner, at a height of 21 mm above the burner surface. The burner was mounted upon a vertical translator, and measurements were made in a region from 3 to 17 mm above the burner surface. Inasmuch as the flame was premixed and one dimensional, it was possible to study the temporal development of the soot-formation processes.

A frequency-doubled pulsed Nd:YAG laser provided 532-nm radiation for all measurements presented in this investigation. We used an aperture with a diameter of 3 mm with which to select a homogeneous part of the laser beam with an original diameter of 10 mm. The difference in the laser pulse energies that are suitable for absorption and LII measurements is orders of magnitude, and the desired energy was reached by means of a variable attenuator.

The extinction measurement was made in a conventional way: The laser light was split into two beams, one of which was directed through the flame while the other acted as a reference beam.[23] The 3-mm beams were vertically focused with $f = 200$ mm cylindrical lenses and monitored on an image-intensified CCD detector. To minimize the influence of small fluctuations in the flames, we averaged 20 accumulations at each measurement height. A detection gate width of 40 ns was used to minimize the influence of background luminosity. There is a general problem in measuring small absorptions with a high accuracy. Often stable continuous lasers are used for this purpose, but in the present measurements a pulsed laser was used. An advantage of using a pulsed laser for absorption measurements is the temporal resolution, and it was with future research in mind that we used a pulsed laser in this investigation. For the accumulated measurements it was estimated that an absorption of 1.0% could be measured with an uncertainty of 10–15%, and in the results from the flame measurements presented here no absorption less than 0.6% was considered. Recently, cavity ringdown spectroscopy was demonstrated to be a useful technique for measuring small absorptions in sooting flames.[33]

For the scattering measurements vertically polarized laser light was focused onto a horizontal sheet over the center of the burner with an $f = 1000$ mm cylindrical lens. As for the extinction measurements, a homogeneous part of the beam was chosen by use of a 3-mm aperture. The laser fluence was of the order of 10^{-3} J/cm^2, thus well below the vaporization limit for soot particles. The scattered light from the flame was monitored with an image intensified CCD detector with a 30-ns gate width. To avoid disturbances, we collected 100 accumulations for each measurement height and used a 532-nm interference filter with 3-nm bandwidth in front of the detector to discriminate background luminosity. To ensure that the measurement was not disturbed by stray light, we compared the scattered signal (Q_{vv}) from nitrogen with the scattered signal from methane. Following literature values, the ratio between these signals should be 2.15.[34] Inasmuch as this value was experimentally verified, we concluded that the contribution from stray light was insignificant. The scattered signal from soot particles was directly calibrated to the scattered signal from nitrogen in consecutive measurements with the identical experimental setup.

The LII signal was generated with a laser energy of ~4.5 mJ/pulse that was focused by a cylindrical lens ($f = 1000$ mm) onto a horizontal sheet above the center of the burner. The thickness of the laser sheet was ~280 μm, which resulted in a corresponding laser fluence of 0.56 J/cm^2. This fluence was in the plateau region, as can be seen from Fig. 1, in which the LII signal is presented as a function of laser fluence for the present experimental setup. A photomultiplier tube detected the resultant LII signal from the sooting flame. Six hundred accumulations of the temporal decay of the LII signal were averaged on a digital oscilloscope with a temporal

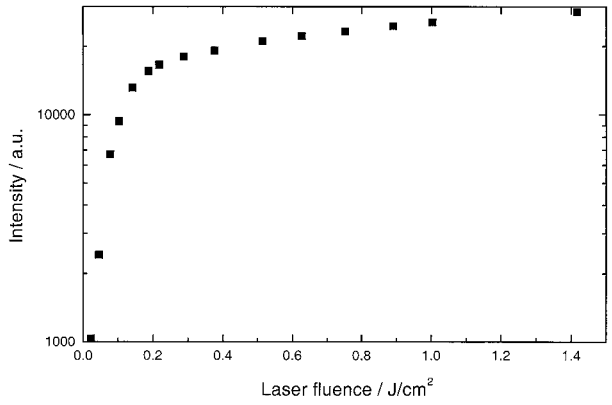

Fig. 1. Incandescence intensity as a function of incident laser fluence for the experimental setup.

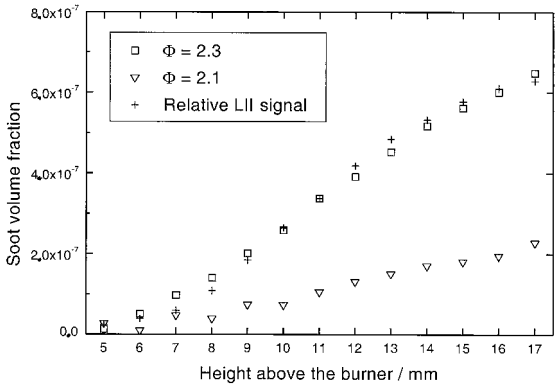

Fig. 3. Soot volume fraction as a function of HAB for the studied flames. The relative LII signal profile is included for the $\Phi = 2.3$ flame, and it has been normalized to the profile derived from absorption measurements at a position of 11 mm.

resolution of 2 ns. An interference filter with a center wavelength of 400 nm and a 10-nm bandwidth was used in front of the detector because such a short detection wavelength strongly reduces the influence of background luminosity. Examples of experimental decay curves for several heights above the burner (HAB) are shown in Fig. 2. A longer signal decay reflects larger soot particles, and higher in the flame the decay time is longer. The experimental signals at 10, 12, and 14 mm gave evaluated primary particle sizes of approximately 9, 14, and 16 nm, respectively. The peaks at 70 and 210 ns are electrical disturbances, which had a negligible influence on the evaluated particle size, as we discuss below.

In the heat-transfer model, a rectangular spatial beam profile was chosen for the laser beam and a Gaussian temporal profile (9 ns FWHM) was used for the pulsed laser. It has been shown that the choice of a rectangular instead of a Gaussian spatial profile has little effect on the evaluated particle diameter.[17] The model was evaluated in the 395–405-nm spectral region. During the growth process a soot particle undergoes significant structural changes as well as changes in chemical composition[35,36] that lead to variations in the refractive index. The refractive index was chosen to be $\mathbf{m} = 1.56–0.46i$,[37] as for the evaluation of the scattering–extinction measurements.

4. Results

The results from the extinction measurements are presented in Fig. 3. Soot volume fractions are presented as a function of HAB, as are the relative LII signals for the equivalence ratio $\Phi = 2.3$. The prompt LII signal corresponds well to the measured soot volume fraction as shown in many previous studies, for example, in Refs. 2, 3, 5, and 13. In Fig. 4 the evaluated soot particle sizes from combined scattering–extinction measurements are shown. These results are important in the following analysis for comparison with soot particle sizes obtained from the time-resolved LII signal. In the calculations, a monodisperse size distribution was assumed and a complex refractive index of $\mathbf{m} = 1.56–0.46i$ (Ref. 37) was chosen. The uncertainties introduced by these assumptions are discussed below.

The particle sizes were evaluated from the time-resolved LII signal during cooling from vaporization temperatures to the ambient-flame temperature. The measured property, the decay time τ, defines the

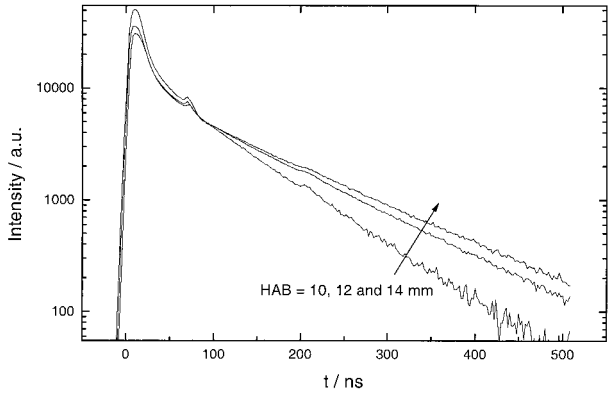

Fig. 2. Experimental decay curves for three HAB values. The curves have been normalized at a time position of 83 ns.

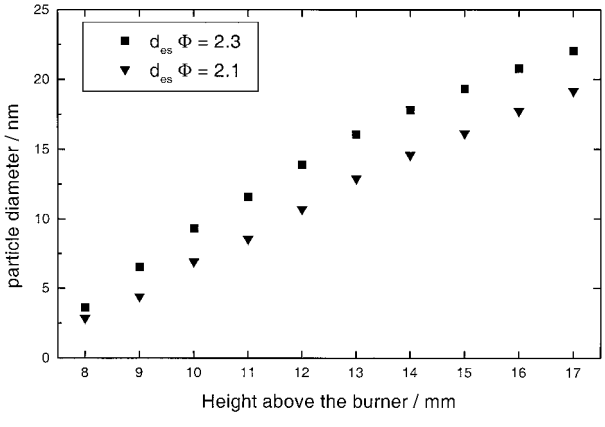

Fig. 4. Evaluated particle diameter from scattering–extinction measurements as a function of HAB for the studied flames.

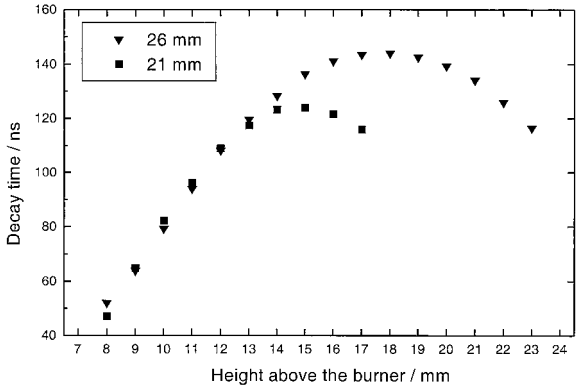

Fig. 5. Decay time as a function of HAB for the flame stabilizer at 21 and at 26 mm above the burner surface.

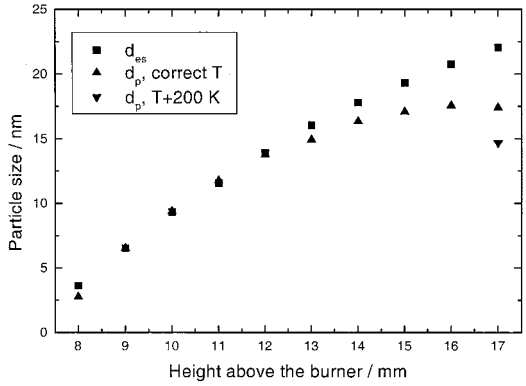

Fig. 6. Particle diameter measured with scattering–extinction (d_{es}) and time-resolved LII (d_p).

time that it takes for the signal to decrease to $1/e$ of its original value. The decay time from the modeled LII signal was fitted to the experimental LII signal between 90 and 550 ns after the peak intensity. Therefore the conduction term rather than the vaporization term dominated the temperature decay. Because a first-order exponential function resulted in a bad fit to the temporal LII signal, most likely because a small amount of vaporization was still occurring, a double-exponential function was used, as described in Ref. 18. During the evaluation it became clear that the short decay time did not contain any significant size information. Thus to reduce the complexity of the double-exponential fit we fixed the short decay time to 20 ns and used the evaluated long decay time as a measure of the particle size.

The decay time was evaluated from measurements at 8–17 mm above the burner in the flame, with the steel plate acting as a flame stabilizer at a 21-mm HAB. It was obvious that the flame stabilizer had significant influence on the flame characteristics, as is illustrated in Fig. 5, which presents the evaluated decay time as a function of HAB for two positions of the stabilizing steel plate, at 21 and 26 mm above the burner. It is evident that the evaluated decay time at lower heights, up to 12-mm HAB, is not influenced by a changed position from 21 to 26 mm of the flame stabilizer. At higher heights the flame conditions change, and the decay time is longer when the steel plate is fixed at a position higher than 26 mm. The result of a longer decay time is generally interpreted as larger soot particles, but, as will be seen in the analysis, the flame temperature will also influence the particle size.

The particle sizes from both scattering–extinction measurements and time-resolved LII are shown in Fig. 6. The volume-equivalent sphere diameter d_{es} is evaluated from the combined scattering–extinction measurements with the assumption of Rayleigh theory, and d_p is evaluated from the temporal profiles of the LII signal. Temperatures measured with CARS were used as input values for the heat-transfer model. It was the variant called dual-broadband rotational CARS that was applied to this flame, and this CARS variant had previously been successfully used for temperature measurements in sooting flames.[38] Evaluated temperatures are expected to have an uncertainty of better than 3% (Ref. 39) in the region of interest (8–17 mm) for which the temperature drops by ~300 K for increasing height.

At low heights in the flame the correspondence between d_{es} and d_p is good. Although there are many uncertainties, as we discuss in Section 4, the similarity of these sizes implies that the aggregation of primary particles to clusters is of minor importance in this region.

At heights above 12 mm the evaluated size from scattering–extinction measurements, d_{es}, deviates from the evaluated primary particle size, d_p. A plausible explanation for this is that the aggregation of soot will have an increasing influence on the soot particle size profiles. Following the research reported in Refs. 5 and 17, the relation between d_{es} and d_p for a cluster of n particles should be $d_{es} = n^{1/3} d_p$, and a comparison of d_{es} and d_p had been made in earlier studies as an attempt to determine the number of primary particles per aggregate.[9] Realizing the importance of knowing the correct temperature for the determination of d_p, we must question the accuracy of such measurements. Although we have knowledge of the temperature in the present flame, a deduced value of the number of primary particles per cluster would have a high uncertainty. It must also be pointed out that neither the extinction measurements of soot volume fraction nor the measurements of d_{es} are temperature dependent, apart from the small influence on the complex refractive index.

An extra point has been added in Fig. 6 at a HAB of 17 mm. This is the evaluated primary particle size with an assumed flame temperature 200 K higher than the temperature of ~1400 K measured with CARS. Thus a 200-K too-high ambient temperature leads to an underestimation of 18% (14.8 instead of 17.5 nm) in the evaluated primary particle size.

4. Discussion

The results in Fig. 6 illustrate uncertainties for the time-resolved LII technique. Also, the scattering–extinction technique has inherent limitations. In what follows, we perform a critical evaluation of sources of errors and of how the errors affect the conclusions that can be drawn from a comparison of evaluated particle sizes for the two techniques.

The refractive index plays a vital role in the determination of both soot volume fraction and particle size by scattering-extinction measurements and has been a subject for discussion.[40] Several refractive-index values are quoted in the literature based on type of soot and measurement technique. Any choice of a complex refractive index of soot will have a large effect on the accuracy of the results. In this investigation we use the refractive index for acetylene soot $\mathbf{m} = 1.56–0.46i$ as determined by Dalzell and Sarofim[37] for our scattering–extinction measurements as well as for the LII model. The use of one value for the refractive index for all experimental cases is not ideal. It has been shown that the value of the refractive index varies with both fuel equivalence ratio and HAB, and this change can be related to changes in chemical composition and temperature of the flame soot.[35] Thus the refractive index differs not only among flames but also within the same flame, causing inaccuracies. The variations of the refractive index within a premixed methane–oxygen flat flame were investigated by Charalampopoulos and Felske.[41] They combined classical light-scattering with dynamic light-scattering measurements and evaluated the refractive index from these measurements. Their results showed, for increasing heights in the flame, an increase in the real part of the complex refractive index from 1.4 to 1.8 and in the imaginary part from 0.4 to 0.8. Although the flames treated in Ref. 41 were different from those that we consider here, we can use their evaluated values to estimate the uncertainty in particle size by choosing one value of the complex refractive index. When the factor $[E(\mathbf{m}))/(F(\mathbf{m})]^{1/3}$ in Eq. 7 of Ref. 41 is evaluated, the value will be in the 0.93–1.24 range for the complex refractive indices at different heights. For $m = 1.56–0.46i$ chosen here, the factor will be 1.07 and thus in the middle of the range. The uncertainty incurred in the evaluated particle size by assumption of a constant value of the refractive index is thus estimated to be as high as 15%, with a possible overestimation at the lowest flame heights that turns into an underestimation higher in the flame.

In the evaluation of particle size from scattering–extinction measurements, a monodisperse particle size distribution is assumed. This has the consequence that the average particle size will be overestimated when the actual size distribution in the flame is polydisperse. The overestimation of d_{es} emanates from the fact that $K_{ext} \sim (\text{particle diameter})^3$ and $Q_{vv} \sim (\text{particle diameter})^6$.[42] A size distribution for the soot particles can also be expected to influence the evaluated particle sizes from LII measurements. In the evaluation of the decay time leading to the determination of d_p, larger particles will incandesce longer and more intensely than smaller particles. This behavior will consequently bias the exponential fit toward larger particles. Particle size distribution can be measured by transmission-electron microscopy following thermophoretic sampling in flames, and a recent publication reported measurement of a standard deviation in primary particle size of 20%.[43]

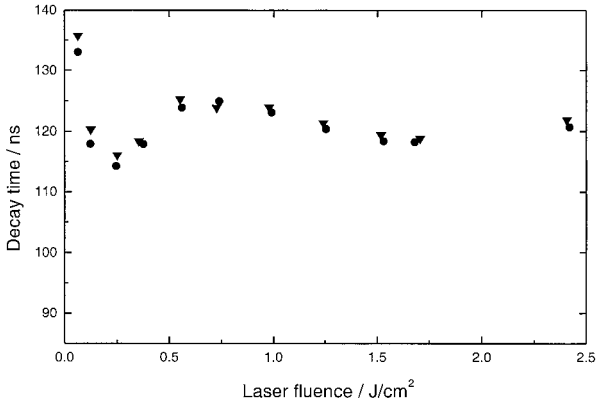

Fig. 7. Fluence dependence of the decay time for two consecutive measurements with identical experimental setup.

The heat-transfer model for laser-heated particles was tested by a theoretical sensitivity analysis similar to that described in Ref. 17. The analysis was based on a 10% increase and decrease of each input parameter in the decay model, and it was performed for a 10-nm and a 20-nm particle. The result was similar to that of Ref. 17 in identifying the ambient gas temperature as the largest source of uncertainty.

A parameter that has a minor influence on the evaluated particle size in sensitivity analysis is laser fluence. However, in the heat-transfer model no morphological changes in the soot as a result of increased laser fluence are taken into consideration. To test this effect we made an experimental study of the variation of decay time as a function of laser fluence for two identical measurements; the results are shown in Fig. 7. It is apparent that low laser fluence below the vaporization limit leads to a longer decay time, in agreement with the results of Ni *et al.*[7] In Fig. 1, where the incandescence signal is presented as a function of laser fluence, there is a distinct transition to a plateau region at ~0.2 J/cm^2. A similar transition to more stable behavior can also be found in Fig. 7 at approximately the same position. It is also interesting to note that the decay time varies with laser fluence, even in the so-called stable region, and introduces a source of error for the evaluated particle diameter. The variation of laser fluence in the plateau region with laser fluences of 0.2–2.5 J/cm^2 gives rise to a 3% uncertainty in the evaluated particle diameter d_p for a particle size of 15 nm.

The two profiles of decay time in Fig. 7 exhibit nearly identical behavior with respect to laser fluence. Although the details of the curves are hard to identify, the cause of the change most probably has to

do with morphological changes in flame soot as a result of laser heating of particles, which have been investigated by Vander Wal *et al*.[14] We have observed that the spatial beam profile influences the measured curves, which may explain why the curve shape in Fig. 7 differs from the curve shape measured by Ni *et al*.[7]

Apart from uncertainties treated in the theoretical sensitivity analysis, some electrical disturbance could be noted in the temporal LII signal in Fig. 2 at 70 and at 210 ns. The electrical disturbance was coupled not to the detected LII signal but to the actual detection process. Inasmuch as the evaluation starts at 90 ns after the laser pulse, these disturbances will not affect the evaluated particle size significantly. By fitting the curves with or without taking the area around 210 ns into account, we found that the error introduced for a 17-nm particle was 0.2% and in a 7-nm particle, 2%.

The precision of the evaluated particle size from LII was also investigated in that 50 single-pulse measurements of the decay curve were evaluated. The relative standard deviation of d_p was 3% for a 17-nm particle, and the mean value corresponded to those of measurements when 600 decay curves were accumulated. This result is encouraging for future measurements. In situations in which accumulated measurements of decay times for particle sizing are impossible, e.g., for turbulent combustion, the only alternative is to perform single-pulse measurements.

An interesting study was recently presented by Vander Wal *et al*. in which particle sizes evaluated from the temporal decay of the LII signal were compared with the sizes evaluated from transmission-electron micrographs.[18] It was observed that the two techniques were in good agreement at flame locations where the soot clusters had an open branched-chain appearance. This observation is important, because it shows that a rather simple heat-transfer model for LII, which, for example, does not take interconnectivity into account, also gives reasonably good results in evaluating primary particle size. It is clear that the present model does not fully explain experimental observations[44] and that further development is needed.

5. Conclusion

In the present study we have investigated the use of laser-induced incandescence (LII) as a tool for soot particle sizing by analyzing the temporal decay of the incandescence signal after laser heating. The particle sizes were evaluated by a comparison of the experimental signal decay with that from a heat-balance model of a laser-heated particle. The study was performed in flat premixed laminar ethylene–air flames, which are well suited for systematic investigations of soot-formation processes by the use of laser diagnostics.

In the lower part of the flame, from soot inception followed by growth to a size of ~12 nm, the particle sizes evaluated by LII were in good agreement with the particle sizes evaluated from scattering–extinction measurements. Although both techniques have inherent uncertainties, the results indicate a low degree of aggregation in this part of the flame.

In the higher part of the flame, where the soot particles had grown to sizes greater than ~12 nm, particle sizes evaluated from LII and scattering–extinction showed a difference that may be explained by increased aggregation. We also realized that knowledge of the temperature is of utmost importance for successful use of this time-resolved LII technique for particle sizing. As an example, an overestimation of the ambient-flame temperature of 14% led to an underestimation of the evaluated particle size of 18%. This determination was supported by a sensitivity analysis performed on the heat-balance model. From the analysis we found that the largest error emanates from uncertainties in the ambient-gas temperature and thus from the initial temperature of the soot particles. There are several limitations on the heat-transfer model for laser-heated particles in its present form; however, for applications in turbulent sooting flames with large fluctuations in temperature, a limiting parameter will still be knowledge of the ambient-flame temperature.

Rotational CARS measurements of temperatures in flames made by Christian Brackmann and Joakim Bood are gratefully acknowledged. We are also thankful for the general interest of and stimulating discussions with Marcus Aldén. This research was financially supported by the Foundation of Strategic Research through the Center for Combustion Science and Technology, the Swedish National Energy Administration, and the Swedish Research Council for Engineering Sciences.

References

1. A. C. Eckbreth, "Effects of laser-modulated particulate incandescence on Raman scattering diagnostics," J. Appl. Phys. **48,** 4473–4479 (1977).
2. L. A. Melton, "Soot diagnostics based on laser heating," Appl. Opt. **23,** 2201–2208 (1984).
3. R. L. Vander Wal and K. J. Weiland, "Laser-induced incandescence: development and characterization towards a measurement of soot-volume fraction," Appl. Phys. B **59,** 445–452 (1994).
4. C. R. Shaddix, J. E. Harrington, and K. C. Smyth, "Quantitative measurements of enhanced soot production in a flickering methane/air diffusion flame," Combust. Flame **99,** 723–732 (1994).
5. B. Quay, T.-W. Lee, T. Ni, and R. J. Santoro, "Spatially resolved measurements of soot volume fraction using laser-induced incandescence," Combust. Flame **97,** 384–392 (1994).
6. P.-E. Bengtsson and M. Aldén, "Soot-visualization strategies using laser techniques," Appl. Phys. B **60,** 51–59 (1995).
7. T. Ni, J. A. Pinson, S. Gupta, and R. J. Santoro, "Two-dimensional imaging of soot volume fraction by the use of laser-induced incandescence," Appl. Opt. **43,** 7083–7091 (1995).
8. R. L. Vander Wal and D. L. Dietrich, "Laser-induced incandescence applied to droplet combustion," Appl. Opt. **3,** 1103–1107 (1995).
9. S. Will, S. Schraml, and A. Leipertz, "Two-dimensional soot-particle sizing by time-resolved laser-induced incandescence," Opt. Lett. **22,** 2342–2344 (1995).

10. C. R. Shaddix and K. C. Smyth, "Laser-induced incandescence-measurements of soot production in steady and flickering methane, propane, and ethylene diffusion flames," Combust. Flame **107,** 418–452 (1996).
11. R. L. Vander Wal, "Onset of carbonization, spatial location via simultaneous LIF–LII and characterization via TEM," Combust. Sci. Technol. **118,** 343–360 (1996).
12. R. L. Vander Wal, "Soot precursor material: visualization via simultaneous LIF–LII and characterization via TEM," in *26th Symposium* (*International*) *on Combustion* (Combustion Institute, Pittsburgh, Pa., 1996), pp. 2269–2275.
13. B. Mewes and J. M. Seitzman, "Soot volume fraction and particle size measurements with laser-induced incandescence," Appl. Opt. **36,** 709–717 (1997).
14. R. L. Vander Wal, T. M. Ticich, and A. B. Stephens, "Optical and microscopy investigations of soot structure alterations by laser-induced incandescence," Appl. Phys. B **67,** 115–123 (1998).
15. M. Braun-Unkhoff, A. Chrysostomou, P. Frank, E. Gutheil, R. Lückerath, and W. Stricker, "Experimental and numerical study on soot formation in laminar high pressure flames," in *27th Symposium* (*International*) *on Combustion* (Combustion Institute, Pittsburgh, Pa., 1998), pp. 1565–1572.
16. S. Will, S. Schraml, and A. Leipertz, "Comprehensive two-dimensional soot diagnostics based on laser-induced incandescence (LII)," in *26th Symposium* (*International*) *on Combustion* (Combustion Institute, Pittsburgh, Pa., 1998), pp. 2277–2284.
17. S. Will, S. Schraml, K. Bader, and A. Leipertz, "Performance characteristics of soot primary particle size measurements by time-resolved laser-induced incandescence," Appl. Opt. **24,** 5647–5658 (1998).
18. R. L. Vander Wal, T. M. Ticich, and A. B. Stephens, "Can soot primary size be determined using laser-induced incandescence," Combust. Flame **116,** 291–296 (1999).
19. J. E. Dec, "A conceptual model of DI diesel combustion based on laser-sheet imaging," in *1997 SAE International Congress and Exposition, Detroit, 24–27 1997* (Society of Automotive Engineers, Warrendale, PA 15096), paper 970873.
20. M. E. Case and D. L. Hofeldt, "Soot mass concentration measurements in diesel engine exhaust using laser-induced incandescence," Aerosol Sci. Technol. **25,** 46–60 (1996).
21. A. D'Alesso, A. Di Lorenzo, A. Borghese, F. Beretta, and S. Masi, "Study of the soot nucleation zone of rich methane-oxygen flames," in *16th Symposium* (*International*) *on Combustion* (Combustion Institute, Pittsburgh, Pa., 1977), pp. 695–708.
22. R. J. Santoro, H. G. Semerjian, and R. A. Dobbins, "Soot particle measurements in diffusion flames," Combust. Flame **51,** 203–218 (1983).
23. P.-E. Bengtsson and M. Aldén, "Application of a pulsed laser for soot measurements in premixed flames," Appl. Phys. B **48,** 155–164 (1989).
24. M. Kerker, *The Scattering of Light and Other Electromagnetic Radiation* (Academic Press, New York, 1969).
25. R. L. Vander Wal and K. A. Jensen, "Laser-induced incandescence: excitation intensity," Appl. Opt. **37,** 1607–1615 (1998).
26. J. D. Black, "Laser induced incandescence measurements of particles in aero-engine exhausts," in *Environmental Sensing and Applications*, M. Carleer, M. Hilton, T. Lamp, R. Reuter, G. M. Russwurm, K. Schaefer, K. Weber, K. Weitkamp, J. P. Wolf, and L. Woppowa, eds., Proc. SPIE **3821,** 209–215 (1999).
27. R. L. Vander Wal, "Laser-induced incandescence: detection issues," Appl. Opt. **35,** 6548–6559 (1996).
28. J. E. Dec, A. O. zur Loye, and D. L. Siebers, "Soot distribution in a D.I. Diesel engine using 2-D laser-induced incandescence imaging," in *1991 SAE International Congress and Exposition, Detroit, 25 February–1 March 1991* (Society of Automotive Engineers, Warrendale, PA 15096), paper 910224.
29. P. N. Tait and D. A. Greenhalgh, "PLIF imaging of fuel fraction in practical devices and LII imaging of soot," Ber. Bunsenges. Phys. Chem. **97,** 1619–1625 (1993).
30. P. Roth and A. V. Filippov, "*In situ* ultrafine particle sizing by a combination of pulsed laser heatup and particle thermal emission," J. Aerosol Sci. **27,** 95–104 (1996).
31. D. R. Snelling, G. J. Smallwood, and ¨O. L. Gülder, "Soot measurement with laser-induced incandescence," presented at the International Energy Agency XIX Task Leaders Meeting on Energy Conservation and Emissions Reduction in Combustion, Capri, Italy, 14–17 September 1997.
32. S. Prucker, W. Meier, and W. Stricker, "A flat flame burner as calibration source for combustion research: temperature and species concentrations of premixed H_2/air flames," Rev. Sci. Instrum. **65,** 2908–2911 (1994).
33. R. L. Vander Wal, "Calibration and comparison of laser-induced incandescence with cavity ring-down," in *27th Symposium* (*International*) *on Combustion* (Combustion Institute, Pittsburgh, Pa., 1998), pp. 59–67.
34. E. D. Landolt-Börnstein, ed., "*Zahlenwerte und Funktionen aus Physik, Chemie, Astronomie, Geophysik und Technik* (Springer-Verlag, Berlin, 1962).
35. T. T. Charalampopoulus, H. Chang, and B. Stagg, "The effects of temperature and composition on the complex refractive index of flame soot," Fuel **68,** 1173–1179 (1989).
36. F. Xu, B. Sunderland, and G. M. Faeth, "Soot formation in laminar premixed ethylene/air flames at atmospheric pressure," Combust. Flame **108,** 471–493 (1997).
37. W. H. Dalzell and A. F. Sarofim, "Optical constants of soot and their application to heat-flux calculations," J. Heat Transf. **91,** 100–104 (1969).
38. P.-E. Bengtsson, L. Martinsson, and M. Aldén, "Rotational CARS thermometry in sooting flames," Combust. Sci. Technol. **81,** 129–140 (1992).
39. L. Martinsson, P.-E. Bengtsson, M. Aldén, and S. Kroll, "A test of different rotational Raman linewidth models: accuracy of rotational coherent anti-Stokes Raman scattering thermometry in nitrogen from 295 to 1850 K," J. Chem. Phys. **99,** 2466–2477 (1993).
40. K. C. Smyth and C. R. Shaddix, "The elusive history of $\mathbf{m} = 1.57 - 0.56i$ for the refractive index of soot," Combust. Flame **107,** 314–320 (1996).
41. T. T. Charalampopoulus and J. D. Felske, "Refractive indices of soot particles deduced from *in-situ* laser light scattering measurements," Combust. Flame **68,** 283–294 (1987).
42. R. A. Dobbins, R. J. Santoro, and H. G. Semerijan, "Interpretation of optical measurements of soot in flames," Prog. Astronaut. Aeronaut. **92,** 208–237 (1984).
43. Ü. Ö. Köylü, C. S. McEnally, D. E. Rosner, and L. D. Pfefferle, "Simultaneous measurements of soot volume fraction and particle size/microstructures in flames using a thermophoretic sampling technique," Combust. Flame **110,** 494–507 (1997).
44. S. Schraml, S. Dankers, K. Bader, S. Will, and A. Leipertz, "Soot temperature measurements and implications for time-resolved laser-induced incandescence (TIRE-LII)," Combust. Flame **120,** 439–450 (2000).